Title: Microstructural white matter changes and links with subcortical structures in chronic schizophrenia: A free-water imaging approach.

Authors: Tiril P. Gurholt[a,b,c*], Unn K. Haukvik[b,d], Vera Lonning[a,c], Erik G. Jönsson[a,e], Ofer Pasternak[f,g†], Ingrid Agartz[a,c,e†]

[a] Norwegian Centre for Mental Disorders Research (NORMENT), Division of Mental Health and Addiction, Institute of Clinical Medicine, University of Oslo, Oslo, Norway.

[b] Norwegian Centre for Mental Disorders Research (NORMENT), Division of Mental Health and Addiction, Oslo University Hospital, Oslo, Norway.

[c] Department of Psychiatric Research, Diakonhjemmet Hospital, Oslo, Norway.

[d] Department of Adult Mental Health, Institute of Clinical Medicine, University of Oslo, Oslo, Norway.

[e] Centre for Psychiatry Research, Department of Clinical Neuroscience, Karolinska Institutet, Stockholm, Sweden.

[f] Department of Psychiatry, Psychiatry Neuroimaging Laboratory, Brigham and Women's Hospital, Harvard Medical School, Boston, MA, USA.

[g] Department of Radiology, Brigham and Women's Hospital, Harvard Medical School, Boston, MA, USA.

[†] Shared senior authorship.

[*] **Corresponding author**: Tiril P. Gurholt, PhD. E-mail: t.p.gurholt@medisin.uio.no, postal address: Oslo University Hospital, P.O.Box 4956 Nydalen, 0424 OSLO, Norway, phone: +47 97 76 27 76.

Abstract

Schizophrenia is a severe mental disorder with often a chronic course. Neuroimaging studies report brain abnormalities in both white and gray matter structures. However, the relationship between microstructural white matter changes and volumetric subcortical structures is not known.

We investigated 30 long-term treated patients with schizophrenia (mean age 51.1±7.9 years, illness duration 27.6±8.0 years) and 42 healthy controls (mean age 54.1±9.1 years) using 3T diffusion and structural magnetic resonance imaging. The free-water imaging method was used to model the diffusion signal, and subcortical volumes were obtained from FreeSurfer. We applied multiple linear regression to investigate associations between (1) patient status and region-based white matter diffusion properties, (2) significant white matter changes and subcortical volumes, and (3) patient white matter diffusion properties with clinical symptoms.

The patients had significantly decreased free-water corrected fractional anisotropy, explained by decreased axial diffusivity and increased radial diffusivity (RD_t) bilaterally in the anterior corona radiata (ACR) and the left anterior limb of the internal capsule compared with controls. In the fornix, the patients had significantly increased RD_t. For the left ACR and fornix there were significant interaction effects between patient status and several of the subcortical structures. In patients, positive symptoms were associated with localized increased free-water and negative symptoms with localized tissue changes. The Cohen's d effect sizes were medium to large (0.61 to 1.20, absolute values).

The results suggest a specific pattern of frontal white matter axonal degeneration and demyelination and fornix demyelination that is linked to subcortical structures in patients with chronic schizophrenia.

Keywords: Psychosis; Brain abnormalities; Deep brain structures; Diffusion tensor imaging; Magnetic resonance imaging.

Introduction

Schizophrenia is a severe and often debilitating mental disorder with largely unknown disease mechanisms. It is well established that patients with schizophrenia, across different disease states, demonstrate white matter microstructural (Kelly et al., 2017) and gray matter structural (van Erp et al., 2016, 2018) changes when compared to healthy controls as well as progressive changes (Dietsche et al., 2017; Kochunov and Hong, 2014; Samartzis et al., 2014) related to the pathophysiology of the disorder and possibly medication use.

Diffusion magnetic resonance imaging (dMRI) and T1-weighted structural imaging are two popular magnetic resonance imaging (MRI) techniques that are often used to study schizophrenia. dMRI, using its popular analysis method - diffusion tensor imaging (DTI) (Basser et al., 1994) - yields in vivo indirect measures of white matter microstructure (Alexander et al., 2007) such as fractional anisotropy (FA), axial diffusivity (AD) and radial diffusivity (RD). The FA measure is purported to be associated with white matter integrity, and can decrease both due to axonal degeneration and demyelination (Mighdoll et al., 2015; Samartzis et al., 2014), indicated by reduced AD and increased RD, respectively (Alexander et al., 2007). However, the FA measure may not provide a good representation of white matter integrity due to several methodological issues (Jones et al., 2013), including that FA is influenced by partial volume effects e.g. from extracellular water contamination and crossing fibers (Alexander et al., 2007). The bi-tensor free-water imaging model (Pasternak et al., 2009) accounts for extracellular free-water, yielding improved tissue specificity of white matter measures compared to the DTI model (Pasternak et al., 2009). The method also provides a free-water fractional volume measure that is affected by extracellular processes e.g. neuroinflammation, atrophy and cellular membrane breakdown (Oestreich et al., 2017).

The largest cross-sectional DTI study to date has shown that patients with schizophrenia have widespread white matter FA reductions, with regionally more severe changes with increasing illness duration (Kelly et al., 2017). Recent cross-sectional free-water imaging studies in schizophrenia corroborate increasing tissue change with illness duration; At schizophrenia onset, reports indicate limited tissue change together with widespread increase in free-water (Lyall et al., 2018; Pasternak et al., 2012), while with chronicity there is evidence of widespread tissue changes together with limited free-water increase (Oestreich et al., 2017; Pasternak et al., 2015) when compared to healthy controls. These findings could indicate a severity gradient and that the temporal disease state needs to be considered in schizophrenia studies of microstructural white matter.

Structural MRI studies of patients with schizophrenia have shown widespread cortical thinning (Rimol et al., 2012, 2010; van Erp et al., 2018), area reduction (Rimol et al., 2012; van Erp et al., 2018), folding abnormalities (Nesvåg et al., 2014) and alterations of subcortical volumes, including smaller hippocampus and amygdala volumes and larger basal ganglia volumes (Haukvik et al., 2015; Rimol et al., 2010; van Erp et al., 2016), compared to healthy controls. Longitudinal studies have indicated, although somewhat inconclusively, increasing cortical thinning with illness duration (Dietsche et al., 2017). A recent large cross-sectional study showed enlargement of the putamen and pallidum volumes with age and illness duration (van Erp et al., 2016). White matter changes in schizophrenia indicated by reduced FA have been linked to cortical thinning in temporal regions, cuneus, frontal gyrus, orbitofrontal cortex (Ehrlich et al., 2014), and cingulate cortex (Koch et al., 2013). Recently cortical thinning was also inversely associated with infracortical white matter anisotropy in adult patients (<50 years of age) (Di Biase et al., 2018). A single study has shown increased mean diffusivity of the left accumbens, and the hippocampus and thalamus bilaterally, in patients (Spoletini et al., 2009). This could indicate patterns of associations between brain regions that are limited to patients with schizophrenia.

In the present study we investigated white matter diffusion properties and relations to subcortical structures. The aims of the study were: (1) to identify differences in microstructural white matter diffusion properties between long-term treated patients with schizophrenia and healthy controls using the free-water imaging method; (2) to investigate whether observed white matter microstructural changes in patients were associated with volumetric measures of subcortical structures; and (3) to investigate putative associations between clinical symptoms and white matter microstructure. In line with prior studies, we expected to observe microstructural white matter changes in patients with chronic schizophrenia together with limited evidence of increased free-water (Oestreich et al., 2017; Pasternak et al., 2015), and microstructural white matter diffusion changes in patients to be linked with volumes of subcortical structures similar to prior cortical findings (Ehrlich et al., 2014; Koch et al., 2013). Similarly, in line with a prior free-water imaging study (Pasternak et al., 2015) we expected microstructural white matter changes in patients to be linked with clinical symptoms.

Material and Methods

Study Population

The subject sample consisted of 30 patients (Schizophrenia [N=22], Schizoaffective disorder [N=8]) and 42 controls, recruited among participants from the HUBIN study at the Karolinska Hospital (Ekholm et al., 2005; Nesvåg et al., 2014), and investigated between 2011 and 2015. Exclusion criteria for all participants were age <18 or >70 years, IQ<70, or previous severe head injury. All participants received oral and written information about the study and signed a written informed consent. The study was approved by the Research Ethics Committee at Karolinska Institutet, Sweden, and was conducted in accordance with the Helsinki declaration.

Clinical Assessment

Patients and controls were assessed by a psychiatrist (EGJ) using the Structured Clinical Interview for DSM-III-R axis I disorders (Spitzer et al., 1988). Diagnosis was based on DSM-IV (American Psychiatric Association, 1995). Symptoms were assessed according to the Scale for the Assessment of Negative Symptoms (SANS) (N. C. Andreasen, 1983) and the Scale for the Assessment of Positive Symptoms (SAPS) (N. C. Andreasen, 1984). Psychosocial functioning was assessed using the split version of the Global Assessment of Function (GAF-S and GAF-F) scale (Pedersen et al., 2007). Age at onset was defined as the age of first verified positive psychotic symptom experience and duration of illness was calculated in years from age at onset to age at MRI. Chlorpromazine equivalent antipsychotic dose (CPZ) was computed (Woods, 2003).

Data acquisition

Patients and controls underwent MRI on the same 3T General Electric Healthcare Discovery MR750 Sigma scanner (General Electric Company, Milwaukee, Wisconsin, USA) equipped with an 8-channel head coil at the Karolinska Institutet and Hospital. The diffusion MRI data was acquired with 10 b_0 volumes and 60 diffusion weighted volumes with b=1000 s/mm^2. The scanning parameters were: 128x128 acquisition matrix, repetition time (TR)=6.0s, echo time (TE)=82.9ms, field of view (FOV)=240mm, flip angle=90° and spatial resolution 0.94x0.94x2.9mm^3. A sagittal T1-weighted BRAVO sequence was acquired with TR=7.9s, TE=3.06s, inversion time (TI)=450ms, flip angle=12°, FOV=240mm and voxel size=0.94x0.94x1.2mm^3. There was no major scanner upgrade or change of instrument during the study period.

MRI Processing

All dMRI's were processed as follows: The brain masks of the first b_0 volume were manually edited to remove non-brain tissue. The dMRI's were corrected for eddy current induced distortions and subject head motion using FSLs EDDY (Andersson and Sotiropoulos, 2016). Automatic detection and correction of motion induced signal dropout (Andersson et al., 2016) was enabled. EDDY outputs rotated b-vectors used in subsequent processing and total per-volume-movement used to calculate the average motion. Following EDDY correction, a bi-tensor diffusion model was fitted using a nonlinear regularized fit to obtain a free-water corrected diffusion tensor representing the tissue compartment and the fractional volume of an isotropic free-water compartment (Pasternak et al., 2009). From the diffusion tensor, a tissue specific scalar measurement of fractional anisotropy (FA_t) was derived using FSLs dtifit. FA_t depends on two independent measures, radial diffusivity (RD_t) and axial diffusivity (AD_t), and they were derived for an additional level of investigation. The scalar measurements of each subject were projected onto a standard FA skeleton using Tract-Based Spatial Statistics (TBSS) (Smith et al., 2006). To do so, the FA images were registered to the ENIGMA-DTI FA template (Jahanshad et al., 2013) that aligns with the Johns Hopkins University (JHU) DTI atlas (Mori et al., 2008) following the ENIGMA-DTI processing protocols (http://enigma.ini.usc.edu/). Forty-four regions of interests (ROIs; see overview in Supplemental Note 1) were extracted. The standard DTI measures of AD, RD and mean diffusivity (MD) were also derived and projected onto the FA skeleton.

All T1-weighted MRI scans were processed using FreeSurfer (Fischl, 2012) version 6.0.0. Briefly, the processing steps include motion correction, bias field correction, brain extraction, intensity normalization and automatic Talairach transformation, with optimized 3T bias field filtration (Zheng et al., 2009). Subcortical volumes were obtained through the subcortical segmentation stream (Fischl et al., 2002), except for the hippocampus and amygdala structures obtained through joint segmentation in FreeSurfer version 6.0.0, development version (Iglesias et al., 2015; Saygin et al., 2017). The extracted bilateral subcortical structures were: hippocampus, amygdala, thalamus, nucleus accumbens, caudate, pallidum, putamen and the lateral ventricle.

Only dMRI's and volumetric structures that passed quality control were included in the analyses (see Supplemental Note 2).

Statistics

The demographic variables of patients and controls were compared using χ^2-test for categorical variables, two-sample t-test for normally distributed and two-sided Wilcoxon rank sum test for non-

normally distributed continuous variables. Normality was assessed using the Shapiro-Wilk's normality test (Royston, 1995).

Multiple linear regression was applied in the main analyses (Model 1) to assess the effect of patient status (patient-control difference) on each extracted white matter ROI while adjusting for sex, age, and average movement in independent models using the *lm*-function in R (version 3.5.0). There were 44 ROIs and four different diffusion maps, yielding 176 separate models. We report the main effect of diagnosis. We conducted follow-up analyses in patients for associations between white matter microstructure and medication effects as indicated by CPZ using a similar model.

For ROIs showing significant diagnostic differences in Model 1, we conducted further analyses to assess potential associations with the volume of subcortical structures in independent models. To do so, we extended Model 1 to include a term for the subcortical volumes and its interaction with patient status (Model 2). We were in particular interested in the interaction term to investigate putative differences between patients and controls in the associations between white matter measures and subcortical volumes. We chose not to include ICV in the model as we were interested in the relations between white matter microstructure and subcortical volumes, and not the relative size itself. The number of investigated ROIs depended on the number of significant ROIs from Model 1. For each model, we report the interaction effect between diagnosis and the volumetric subcortical structure on the white matter ROI.

Among patients, using a model similar to Model 1, we analyzed the association between white matter ROIs and clinical symptoms measured by total SAPS and total SANS. This led to 352 separate models. We report the main effect of total SAPS and SANS scores on the ROIs.

To correct for multiple comparisons, we applied false discovery rate (FDR) correction at $\alpha = 0.05$ (Benjamini and Hochberg, 1995) across all test statistics in the family of tests identified by the respective statistical model. P-values $\leq$ FDR threshold were considered significant, while p-values $\in (\text{FRD threshold}, 0.05)$ were considered trend-significant. The Cohen's d effect size was computed directly from the t-value for categorical variables, and for continuous variables via the partial correlation coefficient, r (Nakagawa and Cuthill, 2007).

Results

Demographic and Clinical Data

Patients had an average age of onset (AAO) of 23.5±4.6 years and an average duration of illness of 27.6±8.0 years. Of the patients, 93.3% received antipsychotic medication (8 first generation, 13 second generation, 7 first and second generation) with an average CPZ doze of 409.8±325.2 mg. Compared to the controls, patients had significantly fewer years of education (p=0.0011). As expected, the patients demonstrated significantly increased symptom burden as assessed with SAPS (p=4.4e-10) and SANS (p=1.8e-13), and significantly decreased functioning as assessed by GAF symptom (p=6.2e-13) and GAF function (p=1.4e-13) score. During the diffusion acquisition the patients moved significantly more than the controls (p=0.0298). There were no significant differences in the other clinical or demographic data (Table 1).

Patient-control differences in diffusion properties

FA_t was significantly lower in patients compared with controls in the right anterior corona radiata (ACR) (d=-0.96, p=0.0002), left ACR (d=-0.74, p=0.0040) and left anterior limb of internal capsule (ALIC) (d=-0.69, p=0.0069) (see Figure 1; Supplemental Table S1). In those regions, FA_t changes were driven by significantly lower AD_t (d=-0.94, d=-0.75 and d=-0.71, respectively) and significantly higher RD_t (d=0.94, d=0.71, and d=0.70, respectively). Furthermore, the RD_t of the fornix was significantly higher for patients (d=0.82, p=0.0015) without any significant or trend-significant changes in FA_t or AD_t for the same ROI. There were no significant changes in free-water between patients and controls (Supplemental Figure S1). The FDR threshold for the family of tests was $p \leq 0.0116$. Follow-up analysis among patients did not show any significant CPZ medication effects on white matter microstructure after FDR correction (Supplemental Table S2).

For comparison, running the same analysis using the standard DTI model showed significant differences between patients and controls only for the right ACR (FA: d=-0.88; RD: d=0.66) (Supplemental Table S3). The FDR threshold for the family of tests was $p \leq 0.0124$.

Association between diffusion measures and subcortical volumes

In ROIs with significant diagnostic differences, we investigated for association between diffusion measures and subcortical volumes identified as significant interaction between subcortical volumes and patient status. This resulted in 160 independent tests and the FDR threshold for the family of tests was p-value$\leq$0.0186.

For the FA_t of left ACR there was a significant interaction of diagnosis with the volumes of the hippocampus (left: d=0.77, p=0.0028; right: d=0.69, p=0.0068), thalamus (right: d=0.68, p=0.0076), amygdala (right: d=0.67, p=0.0084) and putamen (left: d=0.62, p=0.0161; right: d=0.61, p=0.0175) (see Figure 2; Supplemental Table S4). For all those regions, except for putamen, there were also significant interactions with diagnosis for AD_t (*hippocampus* (left: d=0.72; right: d=0.61), *thalamus* (right FA_t: d=0.67), *amygdala* (right: d=0.63)) and RD_t (*hippocampus* (left: d=-0.70; right: d=-0.61), *thalamus* (right: d=-0.66), *amygdala* (right: d=-0.61)). For the putamen, bilaterally, there were trend-level (nominally significant) associations for AD_t and RD_t with similar directionality as for the other structures. In general, for patients, lower measures of left ACR FA_t and AD_t co-occurred with smaller subcortical structures and higher measures co-occurred with larger subcortical structures, while for RD_t higher measures co-occurred with smaller subcortical structures and lower RD_t co-occurred with larger subcortical structures. This pattern differs from the controls, with opposing directionality of effects (see Figure 3).

For the RD_t of the fornix, there were significant interactions between diagnosis and the following subcortical structures; *nucleus accumbens* (left: d=-0.73, p=0.0044) and *hippocampus* (left: d=-0.68, p=0.0083; right: d=-0.66, p=0.0100) (see Figure 4; Supplemental Table S5). The scatterplots showed that for subcortical structures with significant diagnosis interaction on the fornix RD_t, patients and controls had opposing directionality of effects. In general, patients with the higher measures of fornix RD_t also had smaller subcortical structures, and patients with lower fornix RD_t had larger subcortical structures.

For the right ACR and left ALIC there were no significant findings (Supplemental Table S6-S7). For all analyses, the main effect of diagnosis remained significant with the same directionality as in Model 1.

Patient associations with clinical symptoms

Analyses in patients only showed that total SAPS scores were significantly associated with increased free-water on the right posterior thalamic radiation (PTR; d=1.20, p=0.0061) and the left sagittal stratum (SS; d=1.16, p=0.0078), respectively (Supplemental Table S8). Furthermore, in the right ALIC total SANS scores were significantly associated with decreased FA_t (d=-1.14, p=0.0088) and increased RD_t (d=1.20, p=0.0061) (Supplemental Table S9). The FDR threshold for the family of tests was p-value≤ 0.0100.

Discussion

In this study we investigated the relationship between free-water imaging measures and subcortical volumes in patients with long-term treated chronic schizophrenia. The main findings were localized lower white matter anisotropy in patients compared with healthy controls, but no differences in free-water. White matter microstructural differences were associated with subcortical volumes showing different patterns for patients and controls.

The observed reduction in FA_t, driven by a combination of AD_t reduction and RD_t increase, could indicate a pattern of axonal degeneration and demyelination in the frontal white matter in long-term treated chronic schizophrenia patients when compared to controls. In the fornix, the increased RD_t without simultaneous reduced FA_t and AD_t could imply demyelination without axonal degeneration in the patients. The free-water imaging method was more sensitive to patient-control differences in white matter microstructure than the standard DTI model. Our findings were similar to and partly overlapping with previous free-water imaging studies indicating reduced FA_t in cross-hemisphere frontal white matter in patients with schizophrenia (Lyall et al., 2018; Oestreich et al., 2017; Pasternak et al., 2015, 2012), and no free-water increase in the chronic state (Oestreich et al., 2017; Pasternak et al., 2015). The FA_t changes were more pronounced than the reported changes in first episode patients (Lyall et al., 2018; Pasternak et al., 2012). However, the FA_t changes were not as widespread as the previously reported changes in chronic schizophrenia (Oestreich et al., 2017; Pasternak et al., 2015). The differences could be due to the limited sample size in the current study, but could also reflect that our long-term treated chronic schizophrenia sample on average had been ill for 27 years. This is longer than the previous studies, and it is not clearly known how the disorder progress with age and illness duration as captured by dMRI.

The observed interactions between patient-control status and subcortical structures on white matter microstructure for both the left ACR and the fornix, indicate patterns of association between the structures that are different in patients with chronic schizophrenia compared to controls. This is in line with previous studies that show cortical thinning in relation to white matter changes in patients with schizophrenia (Di Biase et al., 2018; Ehrlich et al., 2014; Koch et al., 2013). The results may suggest that volumetric properties of brain anatomical structures are related to disrupted white matter microstructure in schizophrenia. The findings were in the direction of larger subcortical structures being associated with less severe white matter change in patients with chronic schizophrenia, or vice versa. This could point towards a severity gradient in structural changes where less pronounced microstructural changes in patients have weaker diagnosis specific links to

subcortical structures. They could also indicate disease specific patterns of associations between subcortical structures and microstructural white matter properties in chronic schizophrenia, and of disrupted functioning of the limbic system (Catani et al., 2013) and prefrontal connections (Barbas, 2015). The reported findings are in line with the hypothesis of schizophrenia being a disorder of dysconnectivity (Pettersson-Yeo et al., 2011; Schmitt et al., 2011; van den Heuvel and Fornito, 2014). It is well established that the limbic system plays a role in schizophrenia, and subcortical structures of the limbic system have previously been reported as reduced in schizophrenia (van Erp et al., 2016). The current study provides further support for limbic system involvement in the disorder together with links to white matter structures, which need to be further investigated.

Among patients, positive symptoms were significantly associated with increased free-water in the right PTR and left SS. Similarly, negative symptoms were associated with reduced FA_t and increased RD_t in the right ALIC. This is in line with a prior study indicating that positive symptoms are associated with increased free-water and negative symptoms with lower FA_t (Pasternak et al., 2015). Studies using the standard DTI method have also previously indicated that negative and positive symptoms are linked to changes in white matter microstructure (Kelly et al., 2017). The linkage between microstructural white matter changes and clinical symptoms needs further investigation.

There are some limitations for the current study. The cross-sectional design makes it difficult to distinguish cause from effect. Moreover, although the effect sizes are strong, the limited sample size calls for replications in larger independent samples. Strengths of the current study includes a well characterized patient sample that has been characterized with research assessment by one psychiatrist for 12 years, 3T high quality dMRI acquisition, validated and robust analysis methods.

In summary, this study provides further evidence for white matter abnormalities, as well as evidence for altered involvement of subcortical structures with white matter microstructure, in patients with chronic schizophrenia when compared to healthy controls. The microstructural white matter changes indicate a process of frontal axonal degeneration and demyelination, and fornix demyelination in the patients. The observed interaction between subcortical structures and patient-control status on white matter microstructure could indicate disease specific patterns of associations between the structures. To fully capture the linkage between gray and white matter tissue in chronic schizophrenia, future studies are needed.

Acknowledgements

This work was funded by The Swedish Research Council (K2012-61X-15078-09-3, K2015-62X-15077-12-3 and 2017-00949), the regional agreement on medical training and clinical research between Stockholm County Council and the Karolinska Institutet; The Research Council of Norway (grants number 223273); KG Jebsen Foundation; and the National Institutes of Health (R01MH108574).

We thank the study participants and clinicians involved in recruitment and clinical assessment at Karolinska Institutet, Sweden, and Sara Holmqvist, Charlotta Leandersson, Erik Söderman, Rosland Sitnikov (Karolinska Institutet, Sweden), Maja Hjorth-Johansen (University of Oslo, Norway), Stener Nerland (Diakonhjemmet Hospital/University of Oslo, Norway) and Francesco Bettella (Oslo University Hospital, Norway), for their assistance.

Contributors

TPG designed the study in collaboration with OP and IA. TPG did the literature search and drafted the manuscript, and interpreted the data together with OP, UKH and VL. OP contributed with the free-water imaging method. EGJ and IA obtained funding, contributed to data acquisition and study design. All authors contributed to and approved the final manuscript.

Conflict of interests

None.

Table 1: Demographics and clinical variables.

Clinical information[1]	**Patients (N=30)**	**Healthy Controls (N=42)**	**Two-sided t-test, two-sided Wilcoxon rank sum test or χ^2-test**	**p-value**
Women, N (%)	8 (26.7)	13 (30.9)	0.02	0.8954
Age (years)	51.1±7.9	54.1±9.1	-1.43	0.1581
Education (years)	12.9±2.2	15.1±3.1	-3.40	**0.0011**
AAO (years)	23.5±4.6			
DOI at MRI (years)	27.6±8.0			
AP Medicated, N (%)	28 (93.3)			
FGA / SGA / mixed, N	8/ 13 / 7			
CPZ (mg)[2]	409.8±325.2			
Clinical measurements				
SAPS total[2]	9.2±7.9	0.2±0.6	6.24	**4.4e-10**
SANS total[2,3]	27.1±13.8	0.6±0.9	7.36	**1.8e-13**
GAF-S[2]	46.5±10.0	81.7±9.0	-7.20	**6.2e-13**
GAF-F[2]	45.5±8.9	86.7±7.6	-7.40	**1.4e-13**

Notes: Significance threshold p<0.05 indicated in bold. For continuous variables, two-sample t-test was applied for normally distributed data and otherwise two-sided Wilcoxon rank sum test. χ^2-test was applied for categorical data. *Abbreviations:* AAO: Age at onset, AP: antipsychotic medication, CPZ: chlorpromazine equivalent antipsychotic dose, DOI: Duration of Illness, FGA: first generation antipsychotics, GAF: Global Assessment of Functioning, GAF-F: GAF–function scale, GAF-S: GAF-symptom scale, MRI: magnetic resonance imaging, Patients: schizophrenia patients, SAPS: Scale for the Assessment of Positive Symptoms, SANS: Scale for the Assessment of Negative Symptoms, SGA: second generation antipsychotics.

[1] Presented as mean±standard deviation, if not stated otherwise.

[2] Data not normally distributed.

[3] Data normally distributed for patients.

Figure 1: Patient-control differences on all ROIs for the diffusion metrics, FA_t, AD_t and RD_t.

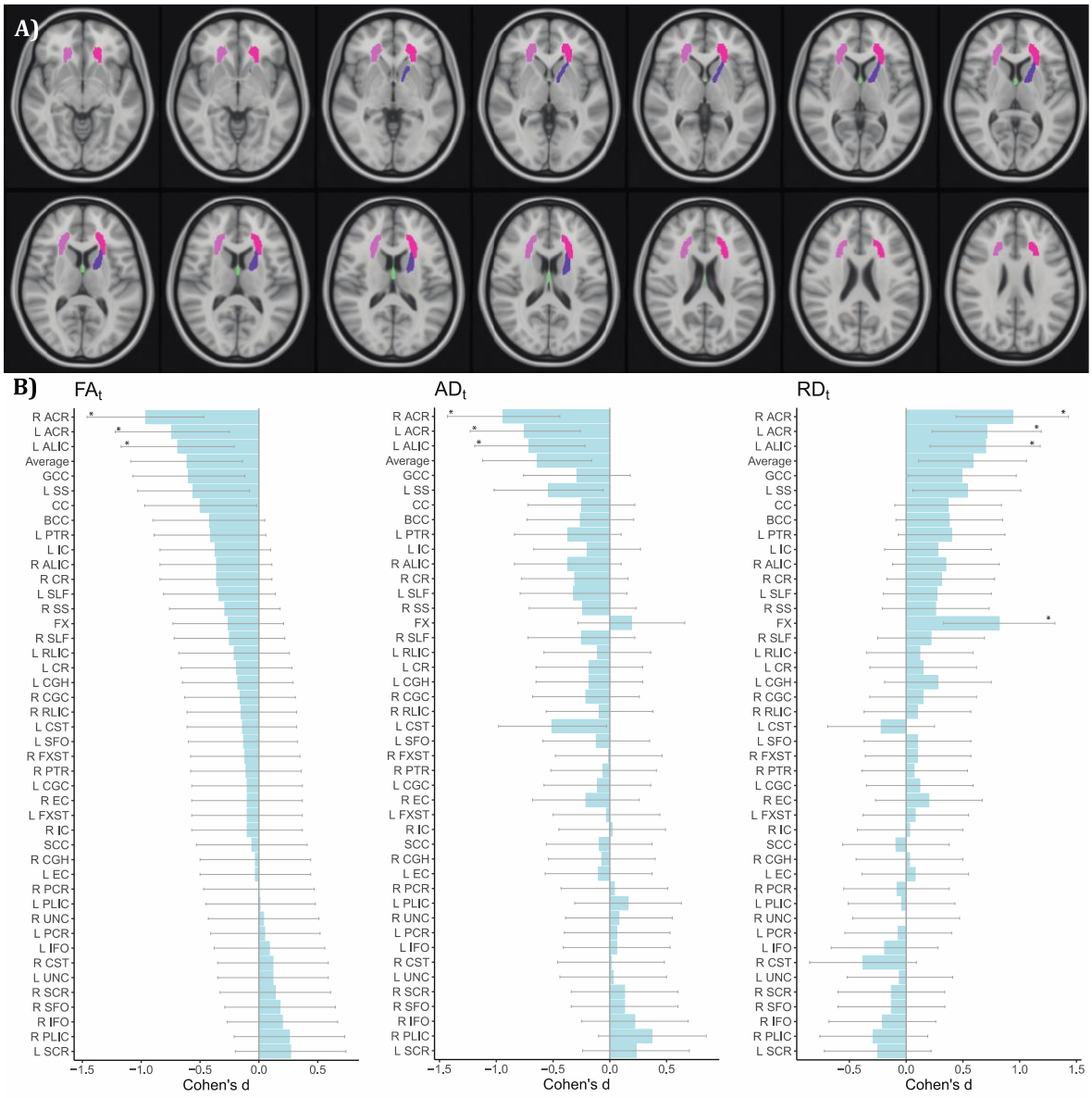

Notes: A) Illustrations of regions of interests with significant patient-control differences: right (light pink), left ACR (pink), left ALIC (purple) and fornix (green) displayed on the MNI 152 T1 atlas in FSL. B) Displays the Cohen's d effect sizes of patient-control differences from regression *Model 1* for FA_t, AD_t and RD_t, on all ROIs, ordered by ascending effect sizes for FA_t. ROIs that pass the FDR threshold of $p \leq 0.0116$ are indicated with *. *Abbreviations:* ACR: anterior corona radiata, AD_t: FW adjusted axial diffusivity, ALIC: anterior limb of internal capsule, Average: average of FA_t, AD_t, RD_t, and FW, respectively. BCC: body of corpus callosum, CC: corpus callosum, CGC: cingulum, CGH: cingulum hippocampal portion, CR: corona radiata, CST: corticospinal tract, EC: external capsule, FA_t: FW adjusted fractional anisotropy, FW: free-water, FX: fornix, FXST: fornix stria terminalis, GCC: genu of corpus callosum, IC: internal capsule, IFO: inferior fronto occipital fasciculus, L: Left, PCR: posterior corona radiata, PLIC: posterior limb of internal capsule, PTR: posterior thalamic radiation, R: Right, RD_t : FW adjusted Radial diffusivity, RLIC: retrolenticular part of IC, ROI: region of interest, SCC: splenium of corpus callosum, SCR: superior corona radiata, SFO: superior fronto-occipital fasciculus, SLF: superior longitudinal fasciculus, SS: sagittal stratum, UNC: uncinate.

Figure 2: Interaction effect between diagnosis and subcortical structures on the left anterior corona radiate.

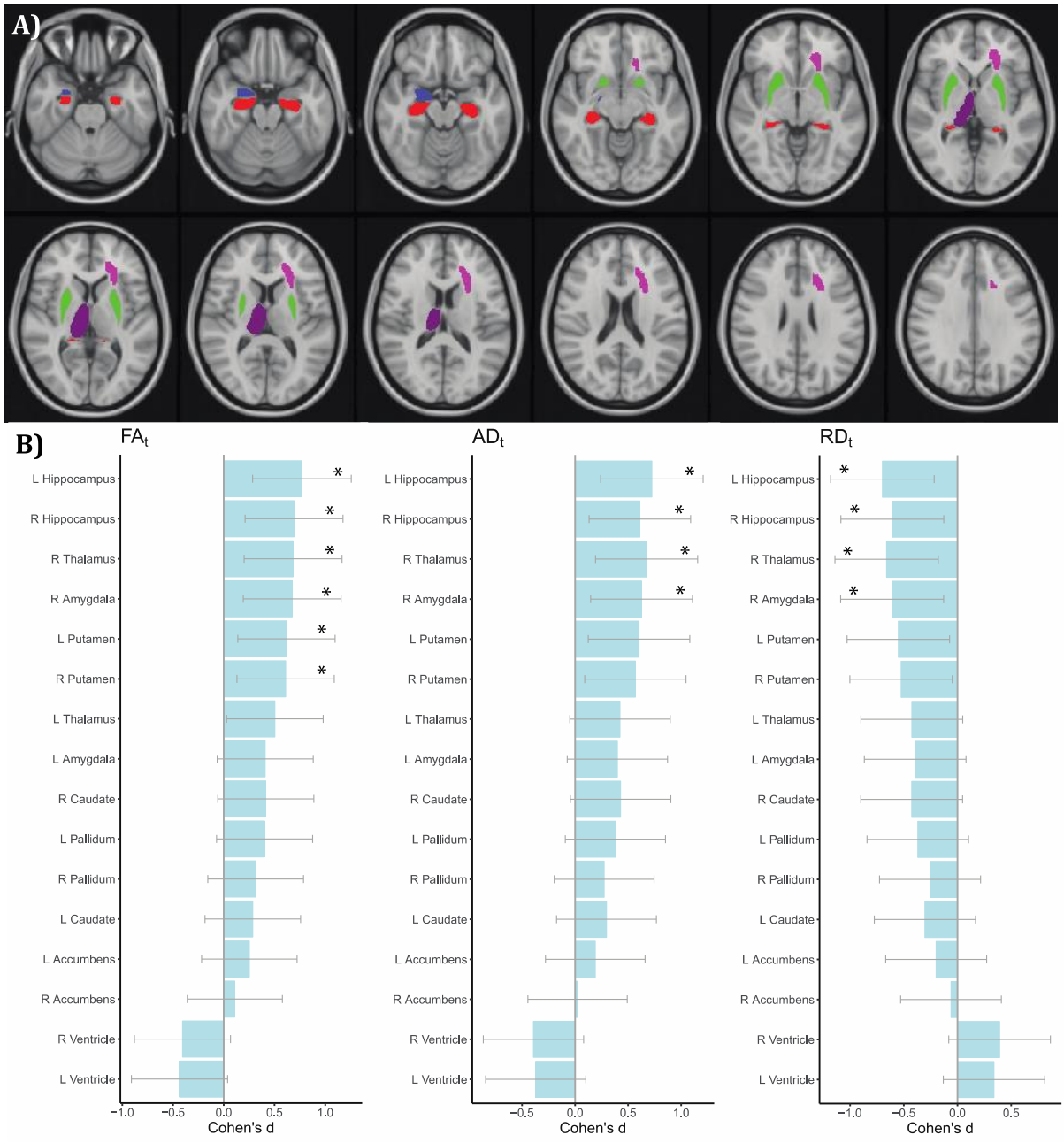

Notes: A) Illustrations of ROIs with significant interactions between diagnosis and subcortical structures on the left ACR: left ACR (pink), left and right hippocampus (red), right amygdala (blue), right thalamus (purple), left and right putamen (green), displayed on the MNI 152 T1 atlas in FSL. B) displays the Cohen's d effect sizes of the interaction term from regression *Model 2* with the left ACR (FA_t, AD_t, RD_t) as the dependent variable. Interactions that pass the FDR threshold of $p \leq 0.0186$ are indicated with *. *Abbreviations:* AD_t: FW adjusted axial diffusivity, ACR: anterior corona radiata, FAt: FW adjusted fractional anisotropy, FW: free-water, L: Left, RD_t: FW adjusted Radial diffusivity, R: Right.

Figure 3: Scatterplots of the left anterior corona radiata with the subcortical structures that have significant interaction with diagnosis.

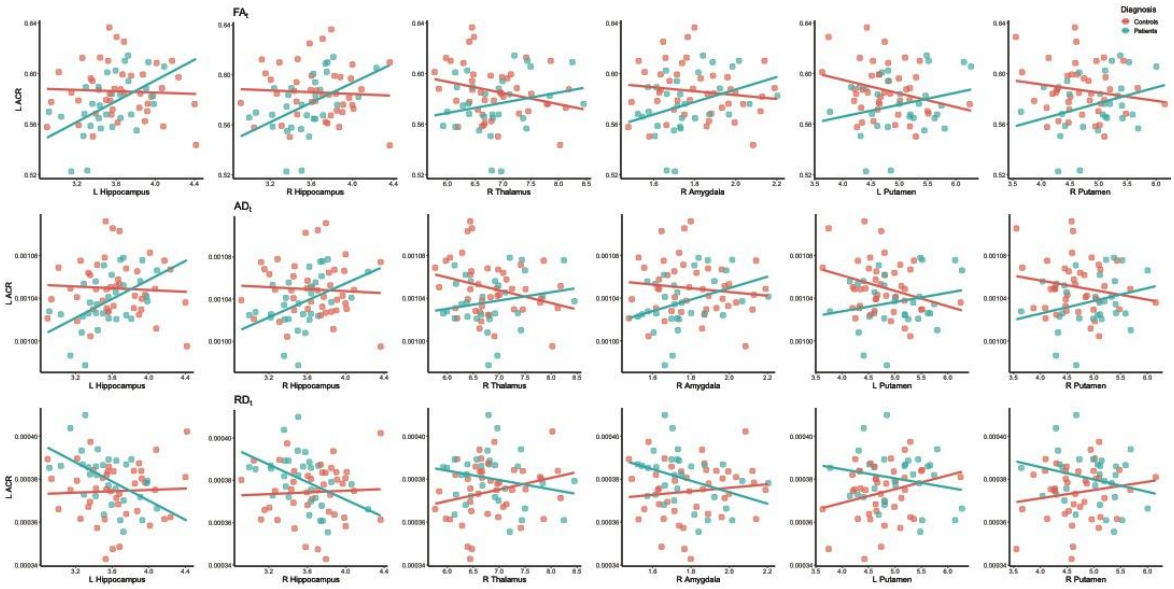

Notes: Top: FA_t of left ACR vs subcortical structures. *Middle*: AD_t of left ACR vs subcortical structures. *Bottom*: Top: RD_t of left ACR vs subcortical structures. Scatterplots are unadjusted for sex, age and average motion. The regression lines are computed separately for patients and controls. *Abbreviations:* AD_t: FW adjusted axial diffusivity, ACR: anterior corona radiata, FA_t: FW adjusted fractional anisotropy, FW: free-water, L: Left, RD_t: FW adjusted Radial diffusivity, R: Right.

Figure 4: The interactions effect of diagnosis with subcortical structures on the fornix.

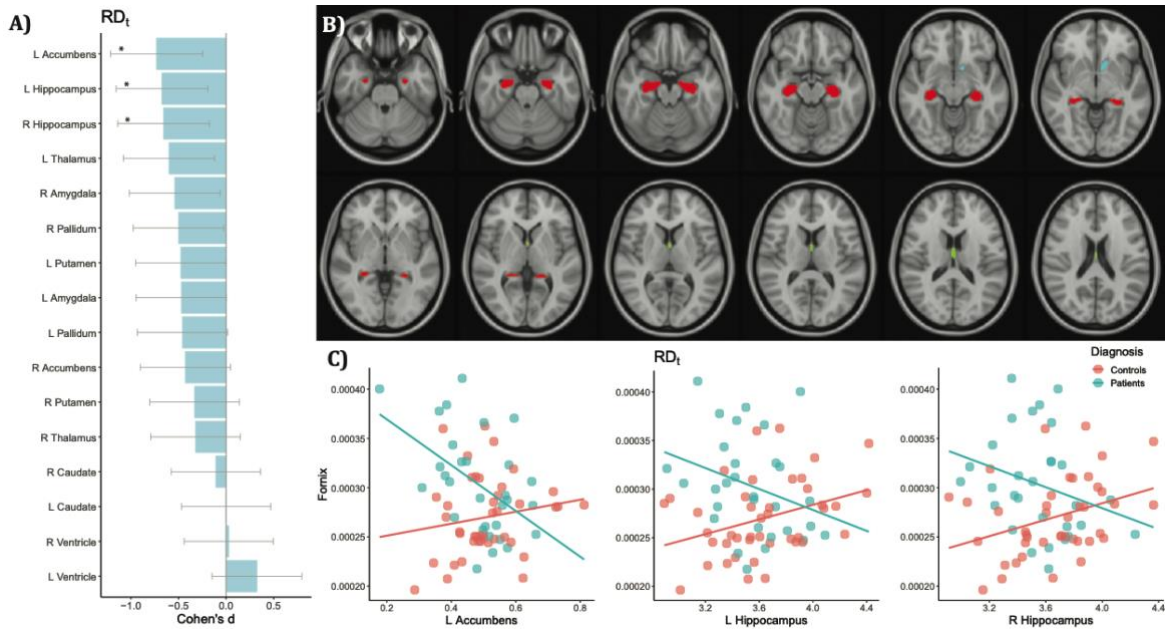

Notes: A) Displays the interaction between diagnosis and subcortical structures on fornix (RD_t). Interactions that pass FDR significance threshold of $p \leq 0.0186$ are indicated with *. B) Illustration of the fornix (green) and the structures with significant interaction displayed on the MNI 152 T1 atlas in FSL; namely left and right hippocampus (red), and left accumbens (cyan). C) Scatterplot for the significant subcortical structures and the fornix (unadjusted). *Abbreviations:* L: Left, RDt: free-water adjusted Radial diffusivity, R: Right.

References

Alexander, A.L., Lee, J.E., Lazar, M., Field, A.S., 2007. Diffusion tensor imaging of the brain. Neurotherapeutics 4, 316–29. https://doi.org/10.1016/j.nurt.2007.05.011

American Psychiatric Association, 1995. Diagnostic and Statistical Manual of Mental Disorders, International Version, Fourth. ed. Washington DC: American Psychiatric Association.

Andersson, J.L.R., Graham, M.S., Zsoldos, E., Sotiropoulos, S.N., 2016. Incorporating outlier detection and replacement into a non-parametric framework for movement and distortion correction of diffusion MR images. NeuroImage 141, 556–572. https://doi.org/10.1016/j.neuroimage.2016.06.058

Andersson, J.L.R., Sotiropoulos, S.N., 2016. An integrated approach to correction for off-resonance effects and subject movement in diffusion MR imaging. NeuroImage 125, 1063–1078. https://doi.org/10.1016/j.neuroimage.2015.10.019

Barbas, H., 2015. General cortical and special prefrontal connections: principles from structure to function. Annu. Rev. Neurosci. 38, 269–289. https://doi.org/10.1146/annurev-neuro-071714-033936

Basser, P.J., Mattiello, J., LeBihan, D., 1994. MR diffusion tensor spectroscopy and imaging. Biophys J 66, 259–67. https://doi.org/10.1016/S0006-3495(94)80775-1

Benjamini, Y., Hochberg, Y., 1995. Controlling the False Discovery Rate - a Practical and Powerful Approach to Multiple Testing. J. R. Stat. Soc. Ser. B-Methodol. 57, 289–300.

Catani, M., Dell'acqua, F., Thiebaut de Schotten, M., 2013. A revised limbic system model for memory, emotion and behaviour. Neurosci Biobehav Rev 37, 1724–37. https://doi.org/10.1016/j.neubiorev.2013.07.001

Di Biase, M.A., Cropley, V.L., Cocchi, L., Fornito, A., Calamante, F., Ganella, E.P., Pantelis, C., Zalesky, A., 2018. Linking Cortical and Connectional Pathology in Schizophrenia. Schizophr. Bull. https://doi.org/10.1093/schbul/sby121

Dietsche, B., Kircher, T., Falkenberg, I., 2017. Structural brain changes in schizophrenia at different stages of the illness: A selective review of longitudinal magnetic resonance imaging studies. Aust. N. Z. J. Psychiatry 51, 500–508. https://doi.org/10.1177/0004867417699473

Ehrlich, S., Geisler, D., Yendiki, A., Panneck, P., Roessner, V., Calhoun, V.D., Magnotta, V.A., Gollub, R.L., White, T., 2014. Associations of white matter integrity and cortical thickness in patients with schizophrenia and healthy controls. Schizophr. Bull. 40, 665–74. https://doi.org/10.1093/schbul/sbt056

Ekholm, B., Ekholm, A., Adolfsson, R., Vares, M., Ösby, U., Sedvall, G.C., Jönsson, E.G., 2005. Evaluation of diagnostic procedures in Swedish patients with schizophrenia and related psychoses. Nord. J. Psychiatry 59, 457–464. https://doi.org/10.1080/08039480500360906

Fischl, B., 2012. FreeSurfer. NeuroImage 62, 774–81. https://doi.org/10.1016/j.neuroimage.2012.01.021

Fischl, B., Salat, D.H., Busa, E., Albert, M., Dieterich, M., Haselgrove, C., van der Kouwe, A., Killiany, R., Kennedy, D., Klaveness, S., Montillo, A., Makris, N., Rosen, B., Dale, A.M., 2002. Whole brain segmentation: automated labeling of neuroanatomical structures in the human brain. Neuron 33, 341–55. http://dx.doi.org/10.1016/S0896-6273(02)00569-X

Haukvik, U.K., Westlye, L.T., Morch-Johnsen, L., Jorgensen, K.N., Lange, E.H., Dale, A.M., Melle, I., Andreassen, O.A., Agartz, I., 2015. In vivo hippocampal subfield volumes in schizophrenia and bipolar disorder. Biol. Psychiatry 77, 581–8. https://doi.org/10.1016/j.biopsych.2014.06.020

Iglesias, J.E., Augustinack, J.C., Nguyen, K., Player, C.M., Player, A., Wright, M., Roy, N., Frosch, M.P., McKee, A.C., Wald, L.L., Fischl, B., Van Leemput, K., Alzheimer's Disease Neuroimaging, I., 2015. A computational atlas of the hippocampal formation using ex vivo, ultra-high resolution MRI: Application to adaptive segmentation of in vivo MRI. NeuroImage 115, 117–37. https://doi.org/10.1016/j.neuroimage.2015.04.042

Jahanshad, N., Kochunov, P.V., Sprooten, E., Mandl, R.C., Nichols, T.E., Almasy, L., Blangero, J., Brouwer, R.M., Curran, J.E., de Zubicaray, G.I., Duggirala, R., Fox, P.T., Hong, L.E., Landman, B.A., Martin, N.G., McMahon, K.L., Medland, S.E., Mitchell, B.D., Olvera, R.L., Peterson, C.P., Starr, J.M., Sussmann, J.E., Toga, A.W., Wardlaw, J.M., Wright, M.J., Hulshoff Pol, H.E., Bastin, M.E., McIntosh, A.M., Deary, I.J., Thompson, P.M., Glahn, D.C., 2013. Multi-site genetic analysis of diffusion images and voxelwise heritability analysis: a pilot project of the ENIGMA-DTI working group. NeuroImage 81, 455–69. https://doi.org/10.1016/j.neuroimage.2013.04.061

Jones, D.K., Knösche, T.R., Turner, R., 2013. White matter integrity, fiber count, and other fallacies: the do's and don'ts of diffusion MRI. NeuroImage 73, 239–254. https://doi.org/10.1016/j.neuroimage.2012.06.081

Kelly, S., Jahanshad, N., Zalesky, A., Kochunov, P., Agartz, I., Alloza, C., Andreassen, O.A., Arango, C., Banaj, N., Bouix, S., Bousman, C.A., Brouwer, R.M., Bruggemann, J., Bustillo, J., Cahn, W., Calhoun, V., Cannon, D., Carr, V., Catts, S., Chen, J., Chen, J. x, Chen, X., Chiapponi, C., Cho, K.K., Ciullo, V., Corvin, A.S., Crespo-Facorro, B., Cropley, V., De Rossi, P., Diaz-Caneja, C.M., Dickie, E.W., Ehrlich, S., Fan, F. m, Faskowitz, J., Fatouros-Bergman, H., Flyckt, L., Ford, J.M., Fouche, J.P., Fukunaga, M., Gill, M., Glahn, D.C., Gollub, R., Goudzwaard, E.D., Guo, H., Gur, R.E., Gur, R.C., Gurholt, T.P., Hashimoto, R., Hatton, S.N., Henskens, F.A., Hibar, D.P., Hickie, I.B., Hong, L.E., Horacek, J., Howells, F.M., Hulshoff Pol, H.E., Hyde, C.L., Isaev, D., Jablensky, A., Jansen, P.R., Janssen, J., Jönsson, E.G., Jung, L.A., Kahn, R.S., Kikinis, Z., Liu, K., Klauser, P., Knöchel, C., Kubicki, M., Lagopoulos, J., Langen, C., Lawrie, S., Lenroot, R.K., Lim, K.O., Lopez-Jaramillo, C., Lyall, A., Magnotta, V., Mandl, R.C.W., Mathalon, D.H., McCarley, R.W., McCarthy-Jones, S., McDonald, C., McEwen, S., McIntosh, A., Melicher, T., Mesholam-Gately, R.I., Michie, P.T., Mowry, B., Mueller, B.A., Newell, D.T., O'Donnell, P., Oertel-Knöchel, V., Oestreich, L., Paciga, S.A., Pantelis, C., Pasternak, O., Pearlson, G., Pellicano, G.R., Pereira, A., Pineda Zapata, J., Piras, F., Potkin, S.G., Preda, A., Rasser, P.E., Roalf, D.R., Roiz, R., Roos, A., Rotenberg, D., Satterthwaite, T.D., Savadjiev, P., Schall, U., Scott, R.J., Seal, M.L., Seidman, L.J., Shannon Weickert, C., Whelan, C.D., Shenton, M.E., Kwon, J.S., Spalletta, G., Spaniel, F., Sprooten, E., Stäblein, M., Stein, D.J., Sundram, S., Tan, Y., Tan, S., Tang, S., Temmingh, H.S., Westlye, L.T., Tønnesen, S., Tordesillas-Gutierrez, D., Doan, N.T., Vaidya, J., van Haren, N.E.M., Vargas, C.D., Vecchio, D., Velakoulis, D., Voineskos, A., Voyvodic, J.Q., Wang, Z., Wan, P., Wei, D., Weickert, T.W., Whalley, H., White, T., Whitford, T.J., Wojcik, J.D., Xiang, H., Xie, Z., Yamamori, H., Yang, F., Yao, N., Zhang, G., Zhao, J., van Erp, T.G.M., Turner, J., Thompson, P.M., Donohoe, G., 2017. Widespread white matter microstructural differences in

schizophrenia across 4322 individuals: results from the ENIGMA Schizophrenia DTI Working Group. Mol. Psychiatry. https://doi.org/10.1038/mp.2017.170 https://www.nature.com/articles/mp2017170#supplementary-information

Koch, K., Schultz, C.C., Wagner, G., Schachtzabel, C., Reichenbach, J.R., Sauer, H., Schlosser, R.G., 2013. Disrupted white matter connectivity is associated with reduced cortical thickness in the cingulate cortex in schizophrenia. Cortex J. Devoted Study Nerv. Syst. Behav. 49, 722–9. https://doi.org/10.1016/j.cortex.2012.02.001

Kochunov, P., Hong, L.E., 2014. Neurodevelopmental and Neurodegenerative Models of Schizophrenia: White Matter at the Center Stage. Schizophr. Bull. 40, 721–728. https://doi.org/10.1093/schbul/sbu070

Lyall, A.E., Pasternak, O., Robinson, D.G., Newell, D., Trampush, J.W., Gallego, J.A., Fava, M., Malhotra, A.K., Karlsgodt, K.H., Kubicki, M., Szeszko, P.R., 2018. Greater extracellular free-water in first-episode psychosis predicts better neurocognitive functioning. Mol Psychiatry 23, 701–707. https://doi.org/10.1038/mp.2017.43

Mighdoll, M.I., Tao, R., Kleinman, J.E., Hyde, T.M., 2015. Myelin, myelin-related disorders, and psychosis. Schizophr. Res. 161, 85–93. http://dx.doi.org/10.1016/j.schres.2014.09.040

Mori, S., Oishi, K., Jiang, H., Jiang, L., Li, X., Akhter, K., Hua, K., Faria, A.V., Mahmood, A., Woods, R., Toga, A.W., Pike, G.B., Neto, P.R., Evans, A., Zhang, J., Huang, H., Miller, M.I., van Zijl, P., Mazziotta, J., 2008. Stereotaxic white matter atlas based on diffusion tensor imaging in an ICBM template. NeuroImage 40, 570–582. https://doi.org/10.1016/j.neuroimage.2007.12.035

N. C. Andreasen, 1984. The Scale for the Assessment of Positive Symptoms (SAPS). University of Iowa, Iowa City, IA.

N. C. Andreasen, 1983. The Scale for the Assessment of Negative Symptoms (SANS). University of Iowa, Iowa City, IA.

Nakagawa, S., Cuthill, I.C., 2007. Effect size, confidence interval and statistical significance: a practical guide for biologists. Biol Rev Camb Philos Soc 82, 591–605. https://doi.org/10.1111/j.1469-185X.2007.00027.x

Nesvåg, R., Schaer, M., Haukvik, U.K., Westlye, L.T., Rimol, L.M., Lange, E.H., Hartberg, C.B., Ottet, M.-C., Melle, I., Andreassen, O.A., Jönsson, E.G., Agartz, I., Eliez, S., 2014. Reduced brain cortical folding in schizophrenia revealed in two independent samples. Schizophr. Res. 152, 333–338. https://doi.org/10.1016/j.schres.2013.11.032

Oestreich, L.K.L., Lyall, A.E., Pasternak, O., Kikinis, Z., Newell, D.T., Savadjiev, P., Bouix, S., Shenton, M.E., Kubicki, M., Australian Schizophrenia Research, B., Whitford, T.J., McCarthy-Jones, S., 2017. Characterizing white matter changes in chronic schizophrenia: A free-water imaging multi-site study. Schizophr Res 189, 153–161. https://doi.org/10.1016/j.schres.2017.02.006

Pasternak, O., Sochen, N., Gur, Y., Intrator, N., Assaf, Y., 2009. Free water elimination and mapping from diffusion MRI. Magn Reson Med 62, 717–30. https://doi.org/10.1002/mrm.22055

Pasternak, O., Westin, C.F., Bouix, S., Seidman, L.J., Goldstein, J.M., Woo, T.U., Petryshen, T.L., Mesholam-Gately, R.I., McCarley, R.W., Kikinis, R., Shenton, M.E., Kubicki, M., 2012. Excessive extracellular volume reveals a neurodegenerative pattern in schizophrenia onset. J Neurosci 32, 17365–72. https://doi.org/10.1523/JNEUROSCI.2904-12.2012

Pasternak, O., Westin, C.F., Dahlben, B., Bouix, S., Kubicki, M., 2015. The extent of diffusion MRI markers of neuroinflammation and white matter deterioration in chronic schizophrenia. Schizophr Res 161, 113–8. https://doi.org/10.1016/j.schres.2014.07.031

Pedersen, G., Hagtvet, K.A., Karterud, S., 2007. Generalizability studies of the Global Assessment of Functioning-Split version. Compr Psychiatry 48, 88–94. https://doi.org/10.1016/j.comppsych.2006.03.008

Pettersson-Yeo, W., Allen, P., Benetti, S., McGuire, P., Mechelli, A., 2011. Dysconnectivity in schizophrenia: Where are we now? Neurosci. Biobehav. Rev. 35, 1110–1124. https://doi.org/10.1016/j.neubiorev.2010.11.004

Rimol, L.M., Hartberg, C.B., Nesvag, R., Fennema-Notestine, C., Hagler, D.J., Pung, C.J., Jennings, R.G., Haukvik, U.K., Lange, E., Nakstad, P.H., Melle, I., Andreassen, O.A., Dale, A.M., Agartz, I., 2010. Cortical thickness and subcortical volumes in schizophrenia and bipolar disorder. Biol. Psychiatry 68, 41–50. https://doi.org/10.1016/j.biopsych.2010.03.036

Rimol, L.M., Nesvag, R., Hagler, D.J., Bergmann, O., Fennema-Notestine, C., Hartberg, C.B., Haukvik, U.K., Lange, E., Pung, C.J., Server, A., Melle, I., Andreassen, O.A., Agartz, I., Dale, A.M., 2012. Cortical volume, surface area, and thickness in schizophrenia and bipolar disorder. Biol. Psychiatry 71, 552–60. https://doi.org/10.1016/j.biopsych.2011.11.026

Royston, P., 1995. Remark AS R94: A Remark on Algorithm AS 181: The W-test for Normality. Appl. Stat. 44, 547–551. https://doi.org/10.2307/2986146

Samartzis, L., Dima, D., Fusar-Poli, P., Kyriakopoulos, M., 2014. White Matter Alterations in Early Stages of Schizophrenia: A Systematic Review of Diffusion Tensor Imaging Studies. J. Neuroimaging 24, 101–110. https://doi.org/10.1111/j.1552-6569.2012.00779.x

Saygin, Z.M., Kliemann, D., Iglesias, J.E., van der Kouwe, A.J.W., Boyd, E., Reuter, M., Stevens, A., Van Leemput, K., McKee, A., Frosch, M.P., Fischl, B., Augustinack, J.C., Alzheimer's Disease Neuroimaging, I., 2017. High-resolution magnetic resonance imaging reveals nuclei of the human amygdala: manual segmentation to automatic atlas. NeuroImage 155, 370–382. https://doi.org/10.1016/j.neuroimage.2017.04.046

Schmitt, A., Hasan, A., Gruber, O., Falkai, P., 2011. Schizophrenia as a disorder of disconnectivity. Eur. Arch. Psychiatry Clin. Neurosci. 261, 150. https://doi.org/10.1007/s00406-011-0242-2

Smith, S.M., Jenkinson, M., Johansen-Berg, H., Rueckert, D., Nichols, T.E., Mackay, C.E., Watkins, K.E., Ciccarelli, O., Cader, M.Z., Matthews, P.M., Behrens, T.E., 2006. Tract-based spatial statistics: voxelwise analysis of multi-subject diffusion data. NeuroImage 31, 1487–505. https://doi.org/10.1016/j.neuroimage.2006.02.024

Spitzer, R.L., Williams, J.B.W., Gibbon, M., First, M.B., 1988. Structured Clinical Interview for DSM-III-R - Patient Version (SCID-P).

Spoletini, I., Cherubini, A., Banfi, G., Rubino, I.A., Peran, P., Caltagirone, C., Spalletta, G., 2009. Hippocampi, Thalami, and Accumbens Microstructural Damage in Schizophrenia: A Volumetry, Diffusivity, and Neuropsychological Study. Schizophr. Bull. 37, 118–130. https://doi.org/10.1093/schbul/sbp058

van den Heuvel, M.P., Fornito, A., 2014. Brain networks in schizophrenia. Neuropsychol. Rev. 24, 32–48. https://doi.org/10.1007/s11065-014-9248-7

van Erp, T.G., Hibar, D.P., Rasmussen, J.M., Glahn, D.C., Pearlson, G.D., Andreassen, O.A., Agartz, I., Westlye, L.T., Haukvik, U.K., Dale, A.M., Melle, I., Hartberg, C.B., Gruber, O., Kraemer, B., Zilles, D., Donohoe, G., Kelly, S., McDonald, C., Morris, D.W., Cannon, D.M., Corvin, A., Machielsen, M.W., Koenders, L., de Haan, L., Veltman, D.J., Satterthwaite, T.D., Wolf, D.H., Gur, R.C., Gur, R.E., Potkin, S.G., Mathalon, D.H., Mueller, B.A., Preda, A., Macciardi, F., Ehrlich, S., Walton, E., Hass, J., Calhoun, V.D., Bockholt, H.J., Sponheim, S.R., Shoemaker, J.M., van Haren, N.E., Pol, H.E., Ophoff, R.A., Kahn, R.S., Roiz-Santianez, R., Crespo-Facorro, B., Wang, L., Alpert, K.I., Jonsson, E.G., Dimitrova, R., Bois, C., Whalley, H.C., McIntosh, A.M., Lawrie, S.M., Hashimoto, R., Thompson, P.M., Turner, J.A., 2016. Subcortical brain volume abnormalities in 2028 individuals with schizophrenia and 2540 healthy controls via the ENIGMA consortium. Mol Psychiatry 21, 585. https://doi.org/10.1038/mp.2015.118

van Erp, T.G.M., Walton, E., Hibar, D.P., Schmaal, L., Jiang, W., Glahn, D.C., Pearlson, G.D., Yao, N., Fukunaga, M., Hashimoto, R., Okada, N., Yamamori, H., Bustillo, J.R., Clark, V.P., Agartz, I., Mueller, B.A., Cahn, W., de Zwarte, S.M.C., Hulshoff Pol, H.E., Kahn, R.S., Ophoff, R.A., van Haren, N.E.M., Andreassen, O.A., Dale, A.M., Doan, N.T., Gurholt, T.P., Hartberg, C.B., Haukvik, U.K., Jorgensen, K.N., Lagerberg, T.V., Melle, I., Westlye, L.T., Gruber, O., Kraemer, B., Richter, A., Zilles, D., Calhoun, V.D., Crespo-Facorro, B., Roiz-Santianez, R., Tordesillas-Gutierrez, D., Loughland, C., Carr, V.J., Catts, S., Cropley, V.L., Fullerton, J.M., Green, M.J., Henskens, F.A., Jablensky, A., Lenroot, R.K., Mowry, B.J., Michie, P.T., Pantelis, C., Quide, Y., Schall, U., Scott, R.J., Cairns, M.J., Seal, M., Tooney, P.A., Rasser, P.E., Cooper, G., Shannon Weickert, C., Weickert, T.W., Morris, D.W., Hong, E., Kochunov, P., Beard, L.M., Gur, R.E., Gur, R.C., Satterthwaite, T.D., Wolf, D.H., Belger, A., Brown, G.G., Ford, J.M., Macciardi, F., Mathalon, D.H., O'Leary, D.S., Potkin, S.G., Preda, A., Voyvodic, J., Lim, K.O., McEwen, S., Yang, F., Tan, Y., Tan, S., Wang, Z., Fan, F., Chen, J., Xiang, H., Tang, S., Guo, H., Wan, P., Wei, D., Bockholt, H.J., Ehrlich, S., Wolthusen, R.P.F., King, M.D., Shoemaker, J.M., Sponheim, S.R., De Haan, L., Koenders, L., Machielsen, M.W., van Amelsvoort, T., Veltman, D.J., Assogna, F., Banaj, N., de Rossi, P., Iorio, M., Piras, F., Spalletta, G., McKenna, P.J., Pomarol-Clotet, E., Salvador, R., Corvin, A., Donohoe, G., Kelly, S., Whelan, C.D., Dickie, E.W., Rotenberg, D., Voineskos, A.N., Ciufolini, S., Radua, J., Dazzan, P., Murray, R., Reis Marques, T., Simmons, A., Borgwardt, S., Egloff, L., Harrisberger, F., Riecher-Rossler, A., Smieskova, R., Alpert, K.I., Wang, L., Jonsson, E.G., Koops, S., Sommer, I.E.C., Bertolino, A., Bonvino, A., Di Giorgio, A., Neilson, E., Mayer, A.R., Stephen, J.M., Kwon, J.S., Yun, J.Y., Cannon, D.M., McDonald, C., Lebedeva, I., Tomyshev, A.S., Akhadov, T., Kaleda, V., Fatouros-Bergman, H., Flyckt, L., Karolinska Schizophrenia, P., Busatto, G.F., Rosa, P.G.P., Serpa, M.H., Zanetti, M.V., Hoschl, C., Skoch, A., Spaniel, F., Tomecek, D., Hagenaars, S.P., McIntosh, A.M., Whalley, H.C., Lawrie, S.M., Knochel, C., Oertel-Knochel, V., Stablein, M., Howells, F.M., Stein, D.J., Temmingh, H.S., Uhlmann, A., Lopez-Jaramillo, C., Dima, D., McMahon, A., Faskowitz, J.I., Gutman, B.A., Jahanshad, N., Thompson, P.M., Turner, J.A., 2018. Cortical Brain Abnormalities in 4474 Individuals With Schizophrenia and 5098 Control Subjects via the Enhancing Neuro Imaging Genetics Through Meta Analysis (ENIGMA) Consortium. Biol Psychiatry. https://doi.org/10.1016/j.biopsych.2018.04.023

Woods, S.W., 2003. Chlorpromazine equivalent doses for the newer atypical antipsychotics. J Clin Psychiatry 64, 663–7.

Zheng, W., Chee, M.W., Zagorodnov, V., 2009. Improvement of brain segmentation accuracy by optimizing non-uniformity correction using N3. NeuroImage 48, 73–83. https://doi.org/10.1016/j.neuroimage.2009.06.039